Study on Thermoacoustic Properties of Ultrasonic Assisted Green Synthesized Fe_3O_4 Nanofluid

Jayashree Sa and Ganeswar Nath*
Department of Physics, Veer Surendra Sai University of Technology, Burla Sambalpur, Odisha
Email:jayashreesa1994@gmail.com,ganeswar.nath@gmail.comi

Abstract

Magnetic iron oxide nanofluids have attracted the attention of researchers due to their various applications in heat transfer, targeted drug delivery, MRI imaging, hyperthermia treatments, etc. This is because of their unique dimensions, high surface area, and specific magnetic properties. The present experimental studies focus on the thermoacoustic properties of magnetite (Fe3O4) water-based nanofluids. The magnetic Fe3O4 nanoparticles were produced by the simple, non-toxic, biocompatible, eco-friendly, and cost-effective green synthesis method using Aloe barbadensis leaf extract. The produced nanoparticles were subjected to various characterization techniques in order to examine their structural, morphological, and compositional characteristics. X-ray diffraction analysis confirmed the nanocrystalline phase of synthesized nanoparticles which are orthorhombic in structure. The spherical form of the produced nanoparticles was seen in scanning electron microscopy pictures. The prepared Fe3O4 nanoparticles exhibit an absorption peak at 301nm according to UV-Visible spectra analysis. Fe3O4 nanoparticles were successfully formed, as evidenced by the appearance of a distinctive absorption band at 581 cm-1 in a Fourier transform infrared spectroscopy analysis. Particle size analysis showed that the prepared nanoparticles have a size below 100nm. Further, the green synthesized magnetite nanoparticles with various concentrations were used to prepare water-based magnetic nanofluids utilizing the ultrasonication method. The produced nanofluids' temperature-dependent thermo-acoustic characteristics were examined through the use of an ultrasonic interferometer. On the basis of thermo-acoustic properties, particle-particle, and particle-fluid interactions are explained.Also, a unique technique for determining the thermal conductivity of nanofluids using ultrasonic velocities has been proposed.

Keywords: green synthesis; Fe3O4 nanofluid; thermoacoustic properties; ultrasonic velocity; adiabatic compressibility; acoustic impedance

1. Introduction

For numerous thermal engineering applications during the past few decades, scientists have worked to create fluids that perform cooling and heating tasks better than traditional fluids. The efficient use of working fluids is one of the finest ways to improve thermal efficiency. Choi's creation of nano-based particles[1] opened up a new way of thinking about enhancing the performance capabilities of traditional fluids. As a result, the dispersion of nanoparticles with enhanced thermo-physical properties can boost the ability of conventional working fluids to transport heat[2,3]. Furthermore, there is rising concern over the usage of traditional nanofluids in heat transfer systems due to the release of hazardous gases and pollution, which in turn raises the global temperature

Corresponding authors: (E-mail: ganeswar.nath@gmail.com)

above pre-industrial levels and causes extreme weather. Additionally, some nanoparticles may be flammable or even pyrophoric, which raises the possibility of mishaps[4].

Strong chemicals may have additional undesirable effects, such as equipment damage and non-biodegradable byproducts[5]. Eco-friendly nanofluids are thus necessary for creating safer chemical goods to eliminate the aforementioned issues. Green technologies aim to protect the environment, preserve natural resources, and implement sustainable practices that lessen the negative effects of human activity[6]. In this way, green nanotechnology makes use of natural resources to reduce or eliminate environmental concerns associated with using nanoparticles while promoting the progressive replacement of traditional nanomaterials.

Kharat et al. used the chemical co-precipitation approach to create nickel ferrite nanoparticles and the ultrasonic velocity method to study the thermoacoustic behaviour of nickel ferrite-H_2O nanofluids[7]. In another report, M. Leena et al. used a wet chemical method to combine pure zinc oxide, cerium-doped zinc oxide, lanthanum-doped zinc oxide, and cerium-lanthanum-doped zinc oxide nanoparticles (NPs) [8]. Additionally, scientists prepared the nanofluids by distributing them in water and thoroughly blending them using an ultrasonic procedure. Similarly, they used an ultrasonic velocity estimation technique to assess the thermal conductivity of ZnO-H_2O nanofluid. Co-precipitation was used by Anu K. et al. [9] to create H_2O-based magnetite nanofluids with various zinc dopings. This work infers and investigates acoustical parameters like mean free path, adiabatic compressibility, acoustic impedance etc. Superparamagnetic cobalt ferrite nanoparticles were created by P. B. Kharat et al. and used to create ferrofluids by dissolving them in ethylene glycol. Similarly, they described the thorough thermoacoustic analysis of the cobalt ferrite-ethylene glycol nanofluids in this study[10]. The ultrasonic conduct of cobalt ferrite nanofluids produced using a co-precipitation technique was investigated by M. Nabeel Rashin et al. [11]

In this context, we used an ultrasonic velocity approach to study the thermo-acoustic behaviour of H_2O -based magnetite nanofluids. The green synthesis technique was used to create the iron oxide nanoparticles. The produced nanoparticles' structural, morphological, and optical analyses were detailed. The present work also evaluated and examined the thermoacoustic characteristics, including ultrasonic Velocity (C), acoustic Impedance (Z), and adiabatic Compressibility (β).

2. Materials and Methods

2.1 Materials

Ferric chloride (anhydrous $FeCl_3$) was purchased from NICE Chemicals (P) Ltd., Kerala, India. Ferrous sulphate heptahydrate ($FeSO_4.7H_2O$) and Sodium hydroxide (NaOH) were purchased from Isochem laboratory, Kerala, India.

2.1 Preparation of Iron oxide nanoparticles by green synthesis method

2.1.1 Preparation of Aloe vera extract

First, we collected garden-fresh aloe vera leaves and carefully cleansed them with distilled water. Almost 26 grams of finely cut leaves were mixed in 150 mL distilled water and stirred at 50°C for 1 hr with a magnetic stirrer. The mixture was filtered using Whatman filter paper after being cooled to room temperature. Finally, the extract was stored at 5–10°C and can be used as a reducing and stabilizing agent.

2.1.2 Synthesis of Fe_3O_4 nanoparticles using Aloe vera leaves extract

Anhydrous $FeCl_3$ and $FeSO_4.7H_2O$ were used as precursors to make iron oxide nanoparticles. To synthesize Fe_3O_4-NPs, a yellowish colloidal solution was made by mixing a 100mL solution of Fe^{3+} and Fe^{2+} in

a 2:1 M ratio with 50mL of aloe vera extract in a 2:1 ratio. Then, under constant stirring, the freshly made 1M of NaOH was added dropwise to the solution. The solution's pH level was raised to 11. The solution was then agitated for 1 hour to homogenize it and ensure that the reaction was completed. The development of iron oxide nanoparticles is indicated by a shift in the colour of the solution from yellowish brown to dark black. A permanent magnet was then used to separate the as-synthesized Fe_3O_4-NPs. The Fe_3O_4-NPs were centrifuged at 3500rpm and deionized water was used to wash them numerous times. For 24 hours, the nanoparticles were dried at 70°C in an oven. For further characterization, the dried material was kept in an airtight container. At room temperature, all of the experiments were carried out.

2.2 Preparation of Iron oxide nanofluid

Distilled water was utilized as the base fluid for the synthesis of iron oxide nanofluid. Here, we've used a stirrer and an ultrasonic bath sonicator to prepare five different concentrations of nanofluid, namely 0.01, 0.02, 0.03, 0.04, and 0.05 vol%. First, in a beaker with 100 ml of water, 51.8 mg of iron oxide nanopowder was weighed and added to prepare 0.01vol%. The prepared solutions were placed in an ultrasonic bath Sonicator and sonicated for 1hr. High-frequency sound waves produced by the sonication effect allow nanoparticles to be well-diffused into the distilled water for better dispersion[5]. After sonication, the solution was then cooled, agitated with a stirrer for 30 minutes, and then kept in an airtight, moisture-free container. The procedure was repeated for nanofluid concentrations of 0.02, 0.03, 0.04, and 0.05.The use of sonication and stirring allows nanoparticles to disperse properly in distilled water which prevented the nanofluid from aggregation.

2.3 Experimental measurement of nanofluid

Here, we used the multi-frequency ultrasonic interferometer to examine the measurement of ultrasonic velocity (Model NF 10X, Mittel Enterprises). It is easy to build and use, and it produces results that are accurate and repeatable. The speed of sound in a liquid may be easily and accurately calculated. This can produce a variety of ultrasonic waves in the medium, ranging in frequency from 1 MHz to 12 MHz. A frequency of 2 MHz has been employed in this. The quartz plate fixed to the bottom of the measurement cell is intended to be excited by the high-frequency generator. On the high-frequency generator, two control knobs are provided for modifying sensitivity regulation and initial tuning the micro-ammeter. A micro-ammeter is supplied to observe the variations in current. A specially made double-walled measurement cell that controls the temperature of a liquid during the experiment. The reflector plate in the cell can be raised or lowered by a specified distance using a tiny micrometre screw that has been placed at the top of the generator. The ultrasonic interferometer's quartz plate mounted to the bottom can be used to measure the ultrasonic velocity. Before turning on the generator, the fixed to the generator, the cell is first filled with the test substance. Standing waves are created in the liquid between the reflector plate and the quartz crystal as a result of the ultrasonic wave moving the normal form toward the crystal until it is reflected from the moving plate. The micrometre is now progressively moved until the anode in the high-frequency generator's current metre displays the maximum value. The total distance 'x' is calculated using a number of these maximum anode current readings that are transmitted. As a result, it provides the wavelength value, which can be determined using the following relation[12]

$$x = n \times \lambda / 2 \quad (1)$$

$$\lambda = 2x/n \quad (2)$$

The following relation can be used to

calculate the iron oxide nanofluid's ultrasonic velocity C once the wavelength has been determined;

$C = f \times \lambda$ ……. (3)

Other acoustical properties, such as Adiabatic compressibility (β), and Acoustical impedance (Z) can be calculated using these ultrasonic velocity measurements.

Thermal conductivity can be calculated from ultrasonic velocity data by the given relation

$K = 2.8(N/V)^{2/3} K_B C$ ……..(4)

Where N = Avogadro number, V= Molar volume of nanofluid, K_B = Boltzmann constant

3. Characterization

BRUKER D8 ADVANCE was utilized to determine the crystallinity of magnetite nanoparticles using the X-ray diffraction (XRD) technique. Cu (Copper) is regarded as the anode material in the diffractometer's CuKα X-ray source, which has a wavelength of 1.54060A°. At a fixed divergent slit at 10°, the diffractograms were obtained with a 2θ variation from 10° to 80°. At 30mA and 40kV, the X-ray tube was set. Iron oxide nanoparticles' peak pattern and crystalline structure have been examined using PANalytical X'PertHigh score software. SEM (HITACHI-SU-3500) at 5 kV, 0.1 torr operating pressure, and 18 mA operating current which causes the sample to become conductive, was used to study the morphology of iron oxide nanoparticles, Fourier Transform Infrared Spectrophotometer (Bruker alpha-II USA) was used to capture the FTIR spectra, which were operated in the transmittance mode and the wavenumber range of 4000-500cm-1. The UV-Visible spectrometer (UV-19001) was used at room temperature to capture the optical absorption spectra[4].

4. Results and Discussion

4.1 X-Ray Diffraction analysis

XRD data analysis of green-produced iron oxide nanoparticles indicated the formation of the nanocrystalline phase. The presence of iron oxide is confirmed by the diffractograms peak pattern at (30.10°, 35.40°, 43.09°, 53.51°, 56.98°, 62.65°, and 74.10°) with increasing X-ray beam intensity (JCPDS file no:01-089-6466). According to Fig. 1, the peaks are indexed with the miller indices (2 2 0), (3 1 1), (4 0 0), (4 2 2), (5 1 1), (4 4 0), and (5 3 3). The orthorhombic structure of iron oxide traces is confirmed by lattice space group-57, whose cell parameters are a = 2.7992, b = 9.4097, and c = 9.4832. The particle size or grain size of iron oxide was determined using the Debye-Scherer formula[13] to confirm its nanoscale size.

$$D_{hkl} = \frac{k\lambda}{\beta_{hkl} \cos\theta_{hkl}} \qquad (5)$$

Where D_{hkl} is the average crystallite size, β_{hkl} is the full-width half maximum (FWHM) intensity[13], k is Scherer's constant having value 0.9; λ is the wavelength of X-ray which is 0.154nm, and θ_{hkl} is the Bragg's angle. The average crystalline size was estimated to be 11 nm based on the computation.

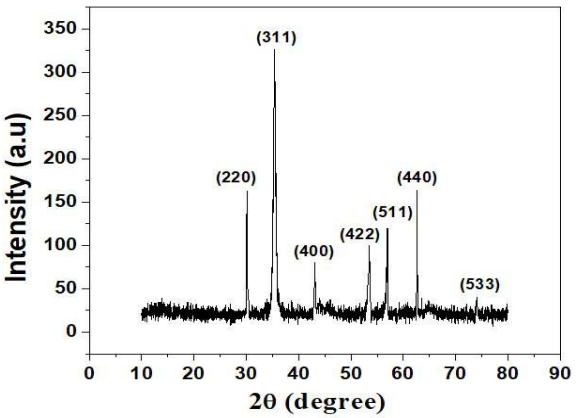

Fig. 1 X-ray diffraction spectra of iron oxide nanoparticle

4.2 SEM Analysis

The SEM revealed that the particles appeared to be smoothly sphere-shaped as shown in Fig.2.Particle diameter measurements following ultrasonication dispersion revealed a normal distribution curve with an axis of 35 nm. More than 95% of the nanoparticles had sizes under 50 nm.

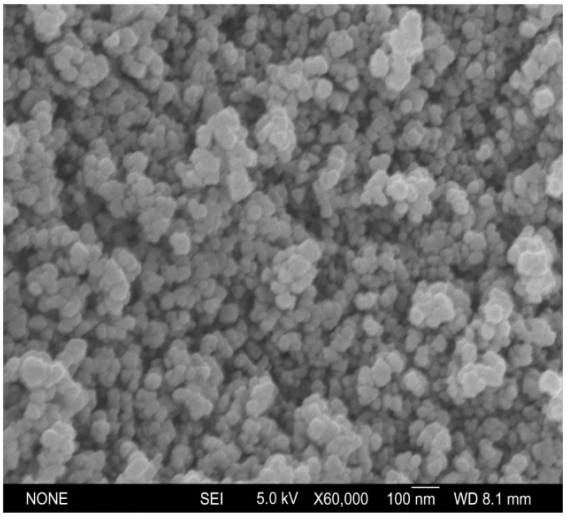

Fig. 2 SEM image of synthesized iron oxide nanoparticle

4.3 FTIR Analysis

FTIR spectroscopy confirms the iron oxide nanofluid synthesis. Infrared radiation was allowed to interact with the iron oxide molecules in the nanofluid. At some quantized frequencies, various bending and stretching vibrations occur. Absorption takes place when the infrared waves are coupled with the vibration of iron oxide molecules. This absorption excites the iron oxide nanoparticles into various excited vibrational states. Through the analyzer, absorption spectra with respect to the wavelength in the range of 400nm to 4000nm were obtained. The stretching and bending bonds of the unknown molecules can be compared with the predefined values for various bonds of known molecules. The prepared sample's absorption spectra are displayed in Fig. 3. The peak at 3314 cm^{-1} indicates the occurrence of the O-H group. The aliphatic C–H peaks appeared at around 2978 cm^{-1}. The stretching vibration of the carbonyl group is observed at 1641cm^{-1}. The peak at about 1054 cm^{-1} is because of C–O bonds[14]. The occurrence of these peaks assures the presence of NPs functionalization with organic compounds. The effect of aqueous leaf extract on Fe_3O_4 NPs results in the formation of coating and stabilization with biological components. Interactions with H_2O molecules improve the functionalization of nanomaterials having hydrophilic groups, such as C-O, carbonyl, and hydroxyl. As a result, nanoparticles become more stable. In between 400-700 cm^{-1}, we have found inorganic lattice vibration. The Fe-O stretching is responsible for the presence of a new sharp peak at around 581 cm^{-1} in Fe_3O_4 NPs[15]. This indicates that magnetite particles were formed by using aloe vera leaf extract.

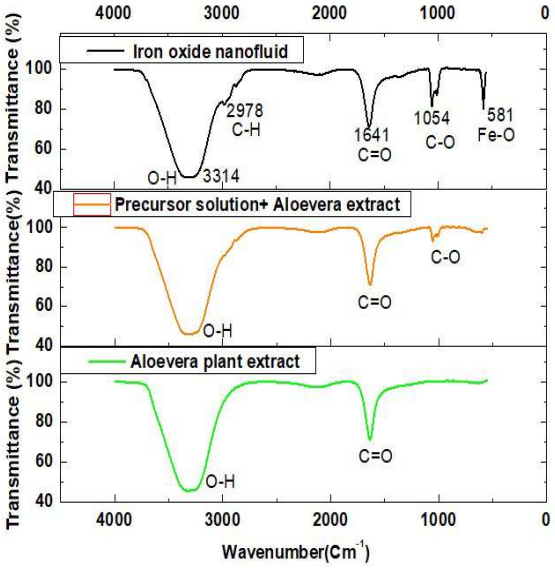

Fig. 3 FTIR of iron oxide nanofluid

4.4 UV-Visible Spectroscopy Analysis

In order to determine the optical characteristics of the iron oxide nanoparticles as well as to conduct a stability study, spectroscopic investigations of the sample were carried out when it was exposed to UV light. Iron oxide nanoparticles' UV-vis spectrum was determined at room temperature and shown in Fig. 4. The production of Fe_3O_4

nanoparticles is shown by the absorbance peak at 301 nm[16].

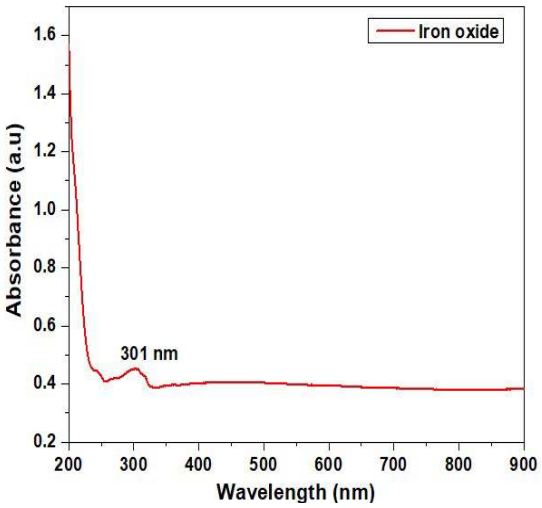

Fig. 4 UV-Visible spectra of Fe_3O_4 nanofluid

4.5 Particle size distribution analysis

Fig. 5 shows the particle size distribution of iron oxide nanofluid, which was carried out using the Malvern Mastersizer -3000[4], which was equipped with an ultrasonic cleaner and a high-intense laser source. The distribution of iron oxide nanoparticles is found to be more uniform with a narrow distribution range, with a particle size range of roughly 1 nm to 60 nm and a mean particle size of 22 nm.

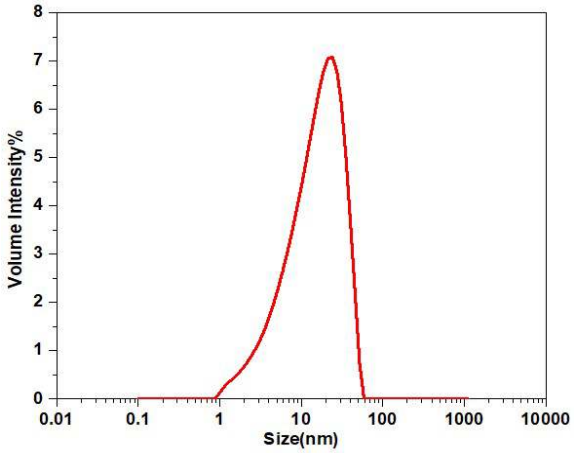

Fig. 5 Particle size distribution of Fe_3O_4 nanofluid

4.6 Thermoacoustic analysis

By using thermoacoustic analysis, we may examine various thermophysical features of the nanofluid by selecting a variety of parameters. We can examine the thermophysical properties of a range of nanofluids by identifying a few important factors from the acoustic analysis. With the available technology, precisely measuring the thermal conductivity of Fe_3O_4 nanofluids has proven to be a challenging task. It's possible that the acoustic investigation is presenting a workable and economical alternative. In light of this, a relationship between temperature and the thermoacoustics parameters of ultrasonic velocity (C), acoustic impedance (Z), and adiabatic compressibility (□) was demonstrated.

4.7 Ultrasonic velocity (C)

Ultrasonic velocity measurements in iron oxide nanofluids can provide crucial details on the liquid's structure, interactions between nanoparticles, the impact of water, the strength of intermolecular association, and the kinetics of molecular activities.Fig. 6 illustrates the ultrasonic velocity of Fe_3O_4 nanofluid as a function of temperature from 30°C to 50°C and volume percentage (0.01-0.05 vol%). It can be shown that when the particle volume fraction rises, the ultrasonic velocity falls off linearly.At room temperature, the ultrasonic velocity in distilledwater is 1512 m/s.As the volume percentage rises from 0.01 to 0.05 vol% at 30°C, the ultrasonic velocity in water-based iron oxide nanofluid falls from 1509 m/s to 1495 m/s. With the rise in temperature from 30°C to 50°C for 0.01 vol%, this velocity rises even more, from 1509 m/s to 1538 m/s. This conclusion confirms the findings of Nabeel Rashin and Hemalatha[17]. who found that temperature increases were associated with an increase in the ultrasonic velocity of the H_2O-based magnetite nanofluid. This is due to the water's open-packed structure being thermally ruptured, which improves the cohesion of the molecules and creates a

less compressible closed-packed form[18], increasing the ultrasonic velocity.

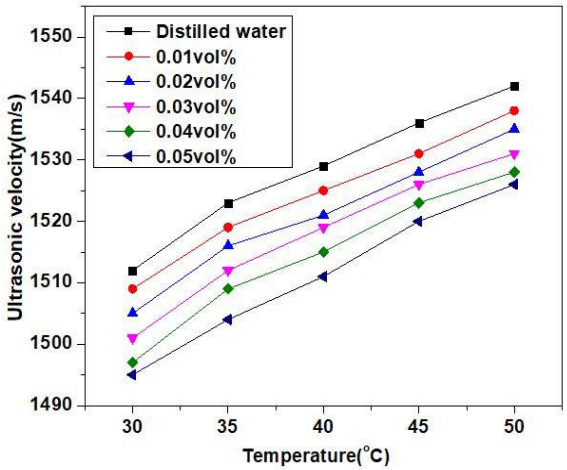

Fig. 6 Variation of the ultrasonic velocity of H_2O-based Fe_3O_4 nanofluid with temperature

4.8 Adiabatic compressibility (β)

The adiabatic compressibility of the Fe_3O_4 nanofluid in proportion to diff. nanoparticle concentrations is shown in Fig. 7.

Using Eq.(6), it was possible to determine the expected value of adiabatic compressibility of Fe_3O_4 nanofluid

$$\beta = 1/\rho C^2 \qquad (6)$$

Where C denotes the ultrasonic velocity, β denotes adiabatic compressibility and ρ denotes the density of Fe_3O_4 nanofluid. The experimental results demonstrate that as the concentration of nanoparticles increased, the compressibility of the nanofluids dropped. In this case, at 30°C the adiabatic compressibility dropped from 4.37×10^{-10} m^2/N (for distilled water), 4.22×10^{-10} m^2/N (for vol. concentration 0.01%), 4.08×10^{-10} m^2/N (for vol. concentration 0.02%) and 3.94×10^{-10} m^2/N (for vol. concentration 0.03%), 3.82×10^{-10} m^2/N (for vol. concentration 0.04%), 3.69×10^{-10} m^2 /N (for vol. concentration 0.05%) and a similar pattern was seen across all temperature measurements. It was also observed that the adiabatic compressibility of 0.05vol% nanofluid decreases from 3.69×10^{-10} m^2/N to 3.55×10^{-10} m^2/N with the rise in temperature from 30°C to 50°C. Increased density suggests that the molecules may be packed closer together and are less likely to repel one another ionically, which may be the cause of the drop in adiabatic compressibility with increasing concentration[19]. This demonstrates that higher concentrations improve binding strength. This drop in compressibility of magnetite nanofluids may be caused by a decrease in the speed of Brownian motion of the fluid molecules due to clustering, which also caused an increase in density and a resistive layer, which lowers the nanofluids' ultrasonic velocity[19].

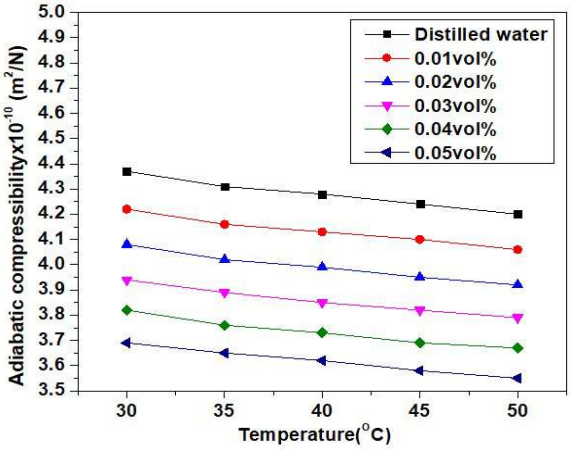

Fig. 7 Variation of Adiabatic compressibility of H_2O-based Fe_3O_4 nanofluid with temperature

4.9 Acoustic impedance (Z)

In Fig. 8, the acoustic impedance of Fe_3O_4 nanofluid in relation to diff. nanoparticle concentrations are depicted. Eq.(7) was used to determine the acoustic impedance of the nanofluid,

$$Z = \rho C \qquad (7)$$

Where Z denotes acoustic impedance, ρ denotes density and C denotes the ultrasonic velocity of the nanofluids. It is evident from the results that as the concentration of nanoparticles increased, so did the nanofluids' acoustic impedance. For instance, when particle concentration

increased from 0.01 to 0.05 vol% at 30 °C, the acoustic impedance increased from 1570 × 10^3 Ns/ m^3 to 1807× 10^3 Ns/ m^3 similar trend was seen across all temperatures. Additionally, a similar pattern was seen for all concentrations as the acoustic impedance increased from 1570 × 10^3 Ns/ m^3 to 1601× 10^3 Ns/ m^3 with an increase in temperature from 30°C to 50°C for 0.01 vol%.

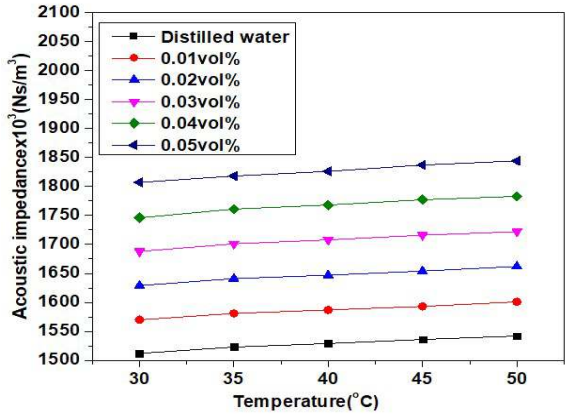

Fig. 8 Variation of Acoustic impedance of H_2O-based Fe_3O_4 nanofluid with temperature

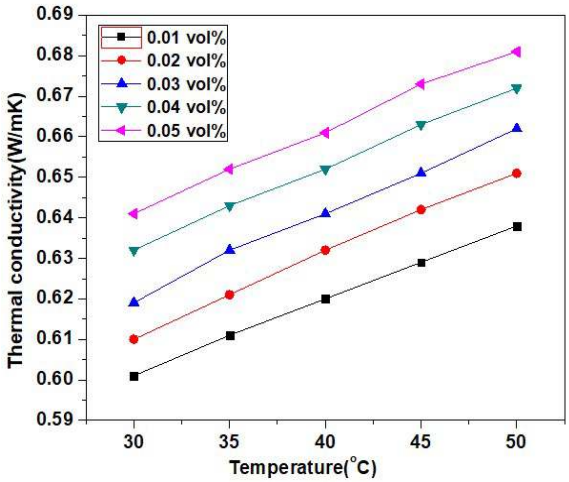

Fig.9 Variation of computed thermal conductivity of H_2O-based Fe_3O_4 nanofluids with temperature

Fig.9 shows how the temperature affects the estimated thermal conductivity of an iron oxide-water nanofluid at different volume concentrations ranging from 0.01% to 0.05%. The figure shows that when temperature and volume concentration rise, thermal conductivity also rises. The loading of nanoparticles at high concentrations causes a rise in Brownian motion with temperature increase, which may be the cause of this large improvement in thermal conductivity. The increase in Brownian motion and subsequent increase in thermal conductivity are caused by the role that micro convection plays in the heat transfer process[20]. Due to the particle's increased frequency of collisions with the base fluid as a result of its Brownian motion, the thermal conductivity and rate of heat transfer are both increased.

5. Conclusion

The thermoacoustic properties of water-based nanofluids comprising Fe_3O_4 nanoparticles was demonstrated in the current work. The green synthesis process was successful in producing magnetite (Fe_3O_4) nanoparticles. The produced Fe_3O_4 nanoparticles' orthorhombic crystal structure and nanocrystalline behaviour were validated by the XRD patterns. The produced iron oxide nanoparticles' spherical shape and nano crystallinity were seen in SEM pictures.The ultrasonic analysis gives the idea about molecular level interactions that take place between the particles and the fluid molecules.The measured acoustical characteristics clearly demonstrate that the molecular interaction was strong in water solvent.This was due tothe stronger bonding between the solute-solvent molecules in the water solvent. Thus, it has been established that there was a significant molecular interaction between the individual molecules in the mixtures. Additionally, a novel method for determining the thermal conductivity of nanofluids using ultrasonic velocity has been put forth. Thermoacoustic investigations provided a viable and affordable option to assess the precise thermophysical parameters. It also shows how the synthesized nanofluids' particle-particle and fluid-particle interfaces interact among them.

Conflicts of interest

The authors declare no conflicts of interest.

Funding

This study received no funding support.

Acknowledgment

The authors are grateful to Hon'ble Vice Chancellor of VSSUT, Burla for giving facilities to carry all types of experiments required for the research work.

References

1) Angayarkanni S & Philip J, Review on thermal properties of nanofluids: recent developments, *Adv Colloid Interface Sci*, **225**(2015) 146–176.
2) Patel J K & Parekh K, Effect of carrier and particle concentration on ultrasound properties of magnetic nanofluids, *Ultrasonics*, **55** (2015) 26–32.
3) Tharayil T, Asirvatham L G, Ravindran V &Wongwises S, Thermal performance of miniature loop heat pipe with graphene–water nanofluid, *Int J Heat Mass Transf,* **93** (2016) 957-968.
4) Sa J & Nath G, Analysis on thermal conductivity of green processed alumina nanofluid for thermal industries, *Advances in Natural Sciences: Nanoscience and Nanotechnologyol,***13** (2022) 025011.
5) Sa J & Nath G, Effect of Green Processing on Enhancement of Thermal Conductivity of Nanofluid for Thermal Applications, *J Sci Ind Res,* **81** (2022) 671-682.
6) Xie X, Zhang Y, He C, Xu T, Zhang B & Chen Q,**.** Bench-scale experimental study on the heat transfer intensification of a closed wet cooling tower using aluminum oxide nanofluids, *Industrial & Engineering Chemistry Research,***56 (**2017) 6022-6034.
7) Kharat P B, Shisode M, Birajdar S, Bhoyar D & Jadhav K, Synthesis and characterization of water-based NiFe2O4 ferrofluid. In: AIP Conference Proceedings, AIP Publishing, (2017) 050122.
8) Leena M & Srinivasan S, Effects of rare earth doped on thermal conductivity of ZnO-water nanofluid by ultrasonic velocity measurements, *Mater Lett*, **219** (2018) 220–224.
9) Anu K &Hemalatha J, Ultrasonic and magnetic investigations of the molecular interactions in zinc doped magnetite nanofluids, *J Mol Liq*, **256** (2018) 213–223.
10) Kharat P B, Shisode M, Birajdar S, Bhoyar D & Jadhav K, Preparation and thermophysical investigations of CoFe2O4-based nanofluid: a potential heat transfer agent. *J Supercond Novel Magn*, (2018) https://doi.org/10.1007/s10948-018-4711-y
11) Rashin M N & Hemalatha J, Ultrasonics—An Effective Non-invasive Tool to Characterize Nanofluids, in Modeling, Methodologies, and Tools for Molecular and Nano-scale Communications, Springer, Berlin (2017)379–399.
12) Paladhi R & Singh R, Miscibility and interaction studies on some aqueous polymer blend solutions by ultrasonic and rheological techniques, *J ApplPolym Sci*, **51**(1994) 1559–1565.
13) Mahdavi M, Namvar F, Ahmad M B & Mohamad R, Green biosynthesis and characterization of magnetic iron oxide (Fe3O4) nanoparticles using seaweed (Sargassum muticum) aqueous extract, *Molecules,***18(5)** (2013) 5954-5964.
14) Demir A, Topkaya R & Baykal A, Green synthesis of superparamagnetic Fe3O4 nanoparticles with maltose: its magnetic investigation, *Polyhedron*, **65** (2013) 282-287
15) Basavegowda N, Magar K B S, Mishra K & Lee Y R, *New J Chem*, **38(11)** (2014)5415-5420.
16) Niraimathee VA, Subha V &RamaswamiSachidanandan ER,*Int J Env Sustain Dev,***15** (2016) 1-227.
17) Rashin M N & Hemalatha J, Magnetic and ultrasonic investigations on magnetite nanofluids. *Ultrasonics*, **52** (2012) 1024-9.
18) Joseph A, Nair P & Mathew S, Investigation of Iron Oxide-Based Ionanofluids and Ionic Liquids by Ultrasonic Sound Velocity Method. *Int J Thermophys*, **41**(2020)1-168.
19) Hemalatha J, Thandapani P & Nalini R, A comparative study on particle–fluid interactions in micro and nanofluids of aluminium oxide, *Microfluidics Nanofluidics*, **10** (2011) 263-270.
20) Haiza H, Yaacob I I&Azhar A Z A, Thermal Conductivity of Water Based Magnetite Ferrofluids at Different Temperature for Heat Transfer Applications, *Solid State Phenom*, **280** (2018) 36–42.